I&EC research
Industrial & Engineering Chemistry Research

Article

Cite This: Ind. Eng. Chem. Res. 2019, 58, 13555−13567

pubs.acs.org/IECR

Online Process Optimization with Active Constraint Set Changes using Simple Control Structures

Dinesh Krishnamoorthy and Sigurd Skogestad*

Department of Chemical Engineering, Norwegian University of Science and Technology (NTNU), Trondheim 7491, Norway

ABSTRACT: The purpose of this paper is to show that online process optimization can be achieved using simple control structures without the need for solving numerical optimization problems online. In particular, we show that changes in active constraint regions can be handled using simple logics such as selectors, without needing to identify the exact location of the active constraint regions a priori, nor using a detailed model online. Good case studies are used to clearly demonstrate how optimal operation can be achieved with changes in active constraint regions using simple feedback control structures.

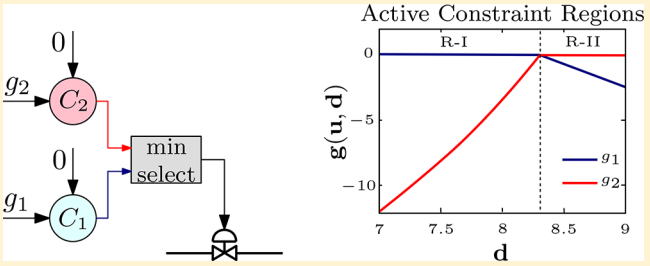

1. INTRODUCTION

The primary objective of online process optimization, also known as real-time optimization (RTO), is to optimize the economic performance, subject to satisfying constraints such as product specifications and operational limits. Online process optimization is traditionally based on rigorous steady-state mathematical models of the process that are used in a numerical optimization solver to compute the optimal inputs and set points.

However, the main challenge with this approach is the need for mathematical models. Mathematical models are generally expensive to obtain and maintain. In addition, the required computation may be difficult to implement and may not converge to the optimal solution. Moreover, there is always plant-model mismatch due to lack of knowledge and/or model simplification. This may lead to suboptimal operation. Addressing the plant-model mismatch has been one of the main focus areas of RTO in the past four decades or so.

Online process measurements are used to cope with plant-model mismatch. The most obvious and common approach in traditional RTO is to update the model using the so-called two-step approach, where deviations between the model predictions and the measurements are used in the first step to update the model parameters. In the second step, the updated steady-state model is used to reoptimize the set points. However, updating the model parameters may not be sufficient to alleviate the effects of model structural mismatch. For example, Roberts and Williams,[1] Marchetti et al.[2] and several others show that it is difficult to achieve the model-adequacy conditions[3] using the two-step model adaptation approach.

Another major challenge with the traditional two-step approach is the steady-state wait time. Because steady-state process models are used, it is necessary for the plant to settle to a new steady-state operating point before updating the model parameters and estimating the disturbances. Darby et al.[4] noted that this steady-state wait time is one of the fundamental limitations of traditional RTO. For processes with long settling times, or with frequent disturbances, the process is operated suboptimally for long periods.

One obvious solution to the steady-state wait time is to use dynamic models for the optimization. However, dynamic RTO has numerical issues and is computationally intensive, even with today's computing power. Other approaches that make use of transient measurements for steady-state optimization have also been recently proposed by Krishnamoorthy et al.[5] and François and Bonvin.[6] For example, the hybrid RTO[5] approach uses a dynamic model and transient measurements for model adaptation and the corresponding static model for optimization. However, all these approaches rely on solving online a numerical optimization problem.

The RTO layer generally has as degrees of freedom, the set points for the controlled variables (CV^{sp}), which is given to the control layer as illustrated in Figure 1. The control layer has degrees of freedom **u**, which are the physical manipulated variables (MV), and in addition to achieving feasible operation, its main objective is to keep the outputs **y** or controlled variables (CV) at the optimal values computed by the RTO layer. The main purpose of this paper is to study how we can eliminate the RTO layer, even for the case when the set of constraints that are active, changes with changing operating conditions. In other words, the objective is to indirectly move the optimization into the control layer.

The idea of achieving optimal operation using feedback control structure dates back to the 80s, where Morari et al.[7] attempted to synthesize a *feedback optimizing control* structure by

Special Issue: Dominique Bonvin Festschrift

Received: January 17, 2019
Revised: May 11, 2019
Accepted: May 16, 2019
Published: May 16, 2019

DOI: 10.1021/acs.iecr.9b00308
Ind. Eng. Chem. Res. 2019, 58, 13555−13567

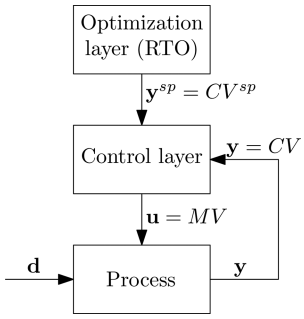

Figure 1. Typical hierarchical decomposition into optimization and control layer.

translating the economic objectives into process control objectives. However, this idea of "feedback optimizing control" from Morari et al.[7] received very little attention, until Skogestad[8] presented the self-optimizing control structure, where the objective is to find a simple feedback control strategy with near-optimal cost, subject to constraints using feedback controllers. Here, Skogestad[8] advocates that it is important to tightly control the constraints that are at its limit at the optimum. In this case, there is no loss by keeping the constraint at its limit (active constraint control). Next, if there are remaining unconstrained degrees of freedom, one should identify suitable controlled variables that translate to the economic objectives. In other words, one should identify the so-called "self-optimizing" control variables. The idea is that controlling the self-optimizing variables at constant set points give an acceptable loss compared to the true optimum, when disturbances occur. Offline optimization is typically needed to find good self-optimizing variables. The ideal self-optimizing variable is the gradient of the cost function, $\mathbf{J_u}$, which should then be controlled to a constant set point of zero,[9] thereby satisfying the *necessary conditions of optimality*.

To summarize, if the optimization problem at hand is an unconstrained problem, then to drive the process to its optimum, we need good models. However, if the problem is constrained such that the optimal operation happens when the constraints are active, then the simplest and most effective approach is to control the active constraints tightly using feedback controllers (active constraint control), without using a model.

In many cases, the active constraint set changes as a function of disturbances. For example, when a disturbance changes, some of the active constraints may no longer be active and some other constraints may become active. A different active constraint set requires reconfiguration of the control loops and also possibly identify different self-optimizing variables for the new operating conditions. This is schematically shown in Figure 2, where the cost function is shown for two different disturbance values d_1 and d_2. The infeasible region is shown in gray shaded area. For disturbance d_1, the optimum occurs when the constraint (shown in red line) is active, whereas, when the disturbance changes to d_2, the constraint is no longer active and a new self-optimizing variable is required, since the problem is now an unconstrained optimization problem. This requires the need to change the controlled variables. This paper focuses on the use of simple control structures to achieve optimal operation, even in the case where the active constraint set changes. Using different example cases, we will show that often simple control logics are sufficient to handle changes in the active constraint sets without needing to use a model online.

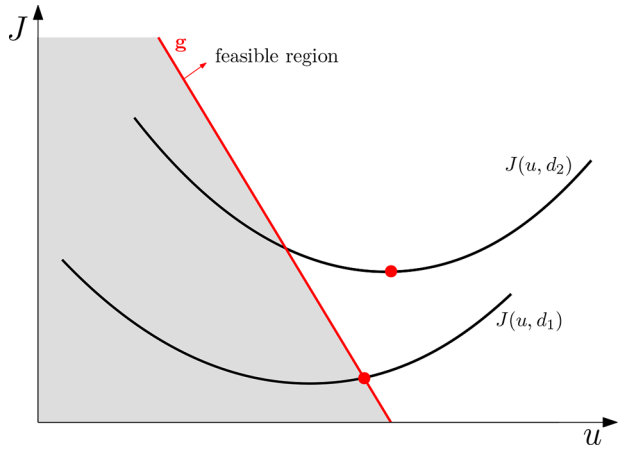

Figure 2. Schematic representation showing the change in the active constraint set for two different disturbances, where for disturbance d_1 the optimum occurs at the constraint, whereas, for disturbance d_2, the optimum is unconstrained.

When we have one manipulated variable (MV) controlling two or more controlled variables (CV), i.e., CV−CV switching, then minimum/maximum selectors can be used. Alternatively, when we have more than one candidate MV to control one controlled variable (CV), then split-range logic can be used. Split range control may also be used when MV−CV pairings need to be changed when a MV saturates. However, this paper focuses on CV−CV switching and the reader is referred to Reyes-Lúa et al.[10] and Reyes-Lúa et al.[11] for more detailed description on MV−MV switching.

The main contribution of this paper is to show that for many simple processes, online *steady-state* process optimization with changes in active CV constraint regions can indeed be achieved by using simple feedback control structures, without having a separate online optimization layer. Some well-known case studies are presented that demonstrate the effectiveness of the proposed control structures and how changes in the active constraint regions can be handled using simple control logics such as selectors.

2. CONTROL STRUCTURE DESIGN FOR ONLINE PROCESS OPTIMIZATION

Consider a steady-state optimization problem

$$\min_{\mathbf{u}} \quad J(\mathbf{u}, \mathbf{d})$$

$$\text{s. t.} \quad \mathbf{g}(\mathbf{u}, \mathbf{d}) \leq 0 \tag{1}$$

where $\mathbf{u} \in \mathbb{R}^{n_u}$ denotes the vector of manipulated variables (MV) and $\mathbf{d} \in \mathbb{R}^{n_d}$ denotes the vector of disturbances, J: $\mathbb{R}^{n_u} \times \mathbb{R}^{n_d} \rightarrow \mathbb{R}$ is the scalar cost function and $\mathbf{g}$: $\mathbb{R}^{n_u} \times \mathbb{R}^{n_d} \rightarrow \mathbb{R}^{n_g}$ denotes the vector of constraints and let $n_a \leq n_g$ denote the number of active constraints at the optimum for a given disturbance $\mathbf{d}$. The Lagrangian of eq 1 is written as

$$\mathcal{L}(\mathbf{u}, \mathbf{d}) = J(\mathbf{u}, \mathbf{d}) + \lambda^T \mathbf{g}(\mathbf{u}, \mathbf{d}) \tag{2}$$

where $\lambda \in \mathbb{R}^{n_g}$ is the vector of Lagrangian multipliers for the constraints. The Karush−Kuhn−Tucker (KKT) optimality conditions for eq 1 state that the necessary condition of optimality is when

DOI: 10.1021/acs.iecr.9b00308
Ind. Eng. Chem. Res. 2019, 58, 13555−13567

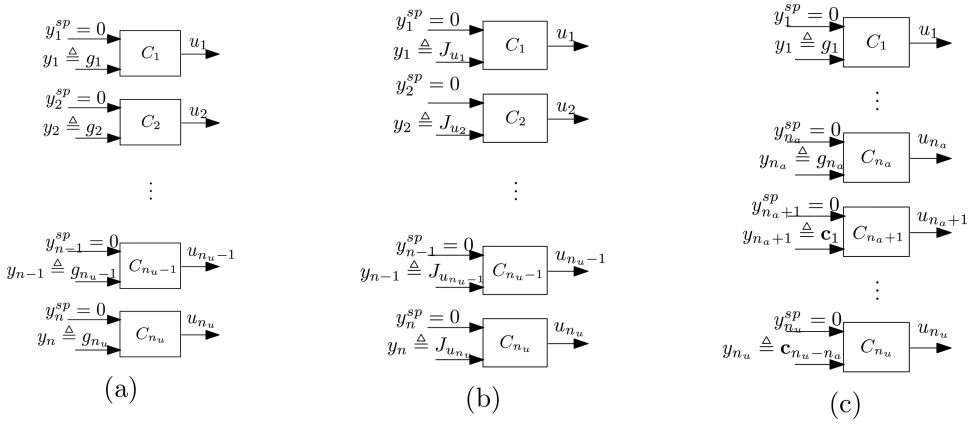

Figure 3. Control structure design for (a) fully constrained case ($n_a = n_u$), (b) fully unconstrained case ($n_a = 0$), and (c) partially constrained case ($0 < n_a < n_u$).

$$\nabla_{\mathbf{u}}\mathcal{L}(\mathbf{u}, \mathbf{d}) = \nabla_{\mathbf{u}}J(\mathbf{u}, \mathbf{d}) + \lambda^T\nabla_{\mathbf{u}}\mathbf{g}(\mathbf{u}, \mathbf{d}) = 0 \tag{3a}$$

$$\mathbf{g}(\mathbf{u}, \mathbf{d}) \leqslant 0 \tag{3b}$$

$$\lambda^T\mathbf{g}(\mathbf{u}, \mathbf{d}) = 0 \tag{3c}$$

$$\lambda \geq 0 \tag{3d}$$

where eq 3b is the primal feasibility, eq 3d is the dual feasibility, and eq 3c is the complementary slackness condition.

Typically, the optimal solution for eq 1 is computed by solving the KKT conditions 3a−3d, either analytically or using numerical methods. However, the objective in this section is to show how to achieve optimal steady-state operation using simple feedback controllers without having to explicitly solve the numerical optimization problem in eq 1. In other words, we aim to translate the KKT conditions into control objectives and thereby move the optimization layer into the control layer.

To achieve this, we need to identify the set of constraints that are active, depending on the disturbances $\mathbf{d}$. By "active constraints", we mean the set of constraints $\mathbf{g}_{\mathbb{A}} \subset \mathbf{g}$, which optimally should be at the limiting value, i.e., $\mathbf{g}_{\mathbb{A}}(\mathbf{u}, \mathbf{d}) = 0$. For each active constraint, we need to find an associated controlled variable, usually simply the constraint itself, i.e., CV $=\mathbf{g}_{\mathbb{A}}$. In some cases, the constraint is on a manipulated variable (MV); in this case one can simply select CV = MV, so actually no controller is needed to control an MV-constraint. Disturbances may cause the active constraints to change, meaning that we get different operating regions (as motivated in Figure 2).

To design controllers that cover the relevant operating regions, the first question one needs to answer is what are the potential combination of active constraints that may be encountered during operation. For a process with n_g constraints, we have a maximum of 2^{n_g} possible combinations of operating regions.[8] To be systematic, we can start our by writing all the possible constraint combinations. But in practice there are often only a few of these combinations that are applicable for a given set of disturbances. Often with good process understanding and "engineering intuition", one can tell a priori which active constraint combinations may be encountered. Hence we eliminate the constraint combinations that are not feasible or not likely.

A more rigorous alternative is to identify using offline optimization, the possible active constraint regions for known disturbances. Once the relevant combination of active constraints are identified, control structures can be designed to handle the different combinations of active constraints. Selecting the right controlled variable is therefore important to achieve optimal operation using simple feedback control structures.

2.1. Selection of Controlled Variables. Depending on the number of active constraints n_a, relative to the number of manipulated variables (MV) n_u, we have four different cases.

Case 1: fully constrained case ($n_a = n_u$). When the number of active constraints at the optimum is equal to the number of MVs (i.e., $n_a = n_u$), then the simplest and easiest approach to achieve optimal operation is to select CV = $\mathbf{g}_{\mathbb{A}}$ and simply maintain the active constraints at their limits using feedback control (active constraint control).[8] Therefore, in this case, we have n_u feedback controllers that controls the $n_u = n_a$ active constraints $\mathbf{y} \triangleq \mathbf{g}_{\mathbb{A}}(\mathbf{u}, \mathbf{d}) = 0$ as shown in Figure 3a.

If a constraint is on the MV, then we do not need any controller at all for this constraint, because the MV can simply be held constant at its limit. More generally, for other constraints, we need to control an associated CV, e.g., CV = $\mathbf{g}_{\mathbb{A}}$ (active constraint control). Active constraint control approach is an old idea and has been used in many examples.[7,11−16] In fact, the example used by Morari et al.[7] in one of the earliest works on feedback optimizing control happened to result in an implementation with controlling the constraints at its limit. Note that in the case of fully constrained optimum, we can achieve optimal operation without using a model for optimization, because the process constraints are usually measured and can be maintained at their limit using feedback.

Case 2: fully unconstrained case ($n_a = 0$). When there are no active constraints at the optimum (i.e., $n_a = 0$), we have n_u unconstrained MVs that can be used to drive the process to its optimum. The optimization problem in eq 1 reduces to

$$\min_{\mathbf{u}} J(\mathbf{u}, \mathbf{d}) \tag{4}$$

because $\mathbf{g}_{\mathbb{A}} = \emptyset$ and the necessary condition of optimality 3 is given by

$$\nabla_{\mathbf{u}}J(\mathbf{u}, \mathbf{d}) = 0 \tag{5}$$

Optimal operation can then be achieved by driving the steady-state gradient $\nabla_{\mathbf{u}}J$ of the cost J from the inputs $\mathbf{u}$ to a constant set point of zero by n_u feedback controllers, thereby fulfilling the necessary conditions of optimality. Therefore, we have n_u

DOI: 10.1021/acs.iecr.9b00308
Ind. Eng. Chem. Res. 2019, 58, 13555−13567

feedback controllers, each controlling the steady-state gradient to a constant set point of 0, i.e,. the controlled variables (CV) $y \triangleq \nabla_{\mathbf{u}} J$ are controlled to a constant set point of $y_{sp} = 0$ as shown in Figure 3b.

There are different ways that can be used to estimate the steady-state gradient $\nabla_{\mathbf{u}} J$. One approach is to use a dynamic model of the process along with the measurements as described by Krishnamoorthy et al.[17] Alternatively, the plant gradients can be estimated directly from the cost measurements (if available) as done in NCO-tracking control[18] and several variants of extremum seeking control.[19−21] The reader is referred to Srinivasan et al.[22] for a comprehensive review of several gradient estimation techniques that can be employed.

Case 3: partially constrained case ($0 < n_a < n_u$). When the number of active constraints at the optimum is less than the number of MVs, we have a partially constrained case. In this case, we first use the n_a available MVs to control the active constraints. For the remaining $(n_u - n_a)$ uncontrolled MVs, we ideally want to control the steady-state cost gradient $\mathbf{J_u}$ to a constant set point such that the KKT conditions in eqs 3a−3d are satisfied.

As mentioned in case 2, in the fully unconstrained case, the steady-state gradients are controlled to a constant set point of zero to fulfill the necessary condition of optimality as shown in eq 5. However, in the partially constrained case, the steady-state gradients $\nabla_{\mathbf{u}} J(\mathbf{u}, \mathbf{d})$ may have to be controlled to a nonzero value to satisfy the KKT conditions. To further explain this, the Lagrangian function 2 of the optimization problem for this particular case reduces down to

$$\mathcal{L}(\mathbf{u}, \mathbf{d}) = J(\mathbf{u}, \mathbf{d}) + \mathbf{g}_{\mathbb{A}}(\mathbf{u}, \mathbf{d})^T \lambda \tag{6}$$

where, $\lambda \in \mathbb{R}^{n_a}$ represents the Lagrange multipliers of the n_a active constraints $\mathbf{g}_{\mathbb{A}}(\mathbf{u}, \mathbf{d})$. Note that the Lagrange multipliers corresponding to the active constraints $\mathbf{g}_{\mathbb{A}}(\mathbf{u}, \mathbf{d})$ are nonzero because of the complementary slackness condition (eq 3c), i.e. $\lambda > 0$. The necessary condition of optimality is then given by

$$\nabla_{\mathbf{u}} \mathcal{L}(\mathbf{u}, \mathbf{d}) = \nabla_{\mathbf{u}} J(\mathbf{u}, \mathbf{d}) + \nabla_{\mathbf{u}} \mathbf{g}_{\mathbb{A}}(\mathbf{u}, \mathbf{d})^T \lambda = 0 \tag{7}$$

$$\nabla_{\mathbf{u}} J(\mathbf{u}, \mathbf{d}) = -\nabla_{\mathbf{u}} \mathbf{g}_{\mathbb{A}}(\mathbf{u}, \mathbf{d})^T \lambda \tag{8}$$

Therefore, the steady-state gradients must be controlled to a constant value equivalent to $-\nabla_{\mathbf{u}} \mathbf{g}_{\mathbb{A}}(\mathbf{u}, \mathbf{d})^T \lambda$ to fulfill the necessary conditions of optimality. However, the expression in eq 8 cannot be used directly for feedback control, because it still contains the Lagrange multiplier, which is an unknown variable. To achieve necessary condition of optimality using feedback controllers, we eliminate the Lagrange multiplier by looking into the nullspace $\mathbf{N}$ of the active constraint gradients $\nabla_{\mathbf{u}} \mathbf{g}_{\mathbb{A}}(\mathbf{u}, \mathbf{d})$.

A shown by Jäschke and Skogestad,[23] $\mathbf{N}$ is defined as the nullspace of $\nabla_{\mathbf{u}} \mathbf{g}_{\mathbb{A}}(\mathbf{u}, \mathbf{d})$ if $\mathbf{N}^T \nabla_{\mathbf{u}} \mathbf{g}_{\mathbb{A}}(\mathbf{u}, \mathbf{d}) = 0$. Because the number of active constraints $n_a < n_u$, Linear inequality constraint qualification (LICQ) is satisfied and therefore, $\nabla_{\mathbf{u}} g_{\mathbb{A}}(\mathbf{u}, \mathbf{d})$ has full row rank. Consequently, the nullspace $\mathbf{N}$ is well-defined. We then have the following theorem:

Theorem 1. Given a steady-state optimization problem (1) with n_u manipulated variables $\mathbf{u}$, n_d independent disturbances $\mathbf{d}$ and n_a active constraints $\mathbf{g}_{\mathbb{A}}(\mathbf{u}, \mathbf{d})$. Let $\mathbf{N} \in \mathbb{R}^{n_u \times (n_u - n_a)}$ be the nullspace of the active constraint gradients $\nabla_{\mathbf{u}} \mathbf{g}_{\mathbb{A}}(\mathbf{u}, \mathbf{d})$, such that $\mathbf{N}^T \nabla_{\mathbf{u}} \mathbf{g}_{\mathbb{A}}(\mathbf{u}, \mathbf{d})^T = 0$. Then the necessary conditions of optimality can be achieved by controlling the linear combination of the gradients

$$\mathbf{c} = \mathbf{N}^T \nabla_{\mathbf{u}} J(\mathbf{u}, \mathbf{d}) \tag{9}$$

to a constant set point of zero.

Proof. To eliminate the Lagrange multiplier, we premultiply eq 8 by $\mathbf{N}^T$ to get

$$\mathbf{N}^T \nabla_{\mathbf{u}} J(\mathbf{u}, \mathbf{d}) = -\mathbf{N}^T \nabla_{\mathbf{u}} \mathbf{g}_{\mathbb{A}}(\mathbf{u}, \mathbf{d})^T \lambda \tag{10}$$

Because $\mathbf{N}$ is in the nullspace of $\nabla_{\mathbf{u}} \mathbf{g}_{\mathbb{A}}(\mathbf{u}, \mathbf{d})$, $\mathbf{N}^T \nabla_{\mathbf{u}} \mathbf{g}_{\mathbb{A}}(\mathbf{u}, \mathbf{d})^T = 0$. Therefore,

$$\mathbf{N}^T \nabla_{\mathbf{u}} J(\mathbf{u}, \mathbf{d}) = -0\lambda \tag{11}$$

by construction, $\mathbf{c}$ is a vector with $(n_u - n_a)$ elements. Hence, to achieve optimal operation, we can then control the $(n_u - n_a)$ elements of the gradient combinations $\mathbf{c}$ to a constant set point of zero using $(n_u - n_a)$ feedback controllers.

To summarize, in the case with $0 < n_a < n_u$, we use n_a MVs to control the active constraints and for the remaining $(n_u - n_a)$ MVs, we control the linear gradient combination $\mathbf{c} = \mathbf{N}^T \nabla_{\mathbf{u}} J(\mathbf{u}, \mathbf{d})$ to a constant set point of zero as shown in Figure 3c. This is similar to null-space method proposed by Alstad and Skogestad,[24] but instead of choosing a linear combination of measurements $\mathbf{c} = \mathbf{H}\mathbf{y}$, we choose a linear combination of the cost gradients as the self-optimizing variable.

Because this self-optimizing variable is computed on the basis of $\mathbf{g}_{\mathbb{A}}(\mathbf{u}, \mathbf{d}) = 0$, it is only valid in this particular active constraint region. Therefore, the control loops tracking the gradient combinations $\mathbf{c} = \mathbf{N}^T \nabla_{\mathbf{u}} J(\mathbf{u}, \mathbf{d})$ using the unconstrained MVs are turned off in the regions other than where it is designed for and the neighboring regions (a neighboring region is an operating region where only one controlled variable (constraint) has changed).[25] Therefore, it is not necessary (and in fact it will be incorrect) to track the unconstrained CVs in all other regions. It is only necessary (and correct) to track the variable $\mathbf{c}$ in the regions where it is active and its neighboring regions.

Case 4: overconstrained case ($n_a > n_u$). If the number of active constraints becomes larger than the number of MVs, then the problem becomes infeasible, because we do not have sufficient MVs to control all the active constraints. In this case, the only possible solution would be to give up controlling less important constraints. This is analogous to using soft constraints on less important constraints to avoid infeasibility issues in numerical optimization problems. In this case, a priority list can be used to determine the less important constraints and only the first n_u constraints are controlled at their limit using feedback controllers. The remaining $(n_a - n_u)$ CV constraints are given up. The control structure in this case would remain the same as shown in Figure 3a. The reader is referred to Reyes-Lúa et al.[10] for a typical priority list that is commonly used. Note that MV hard constraints, for example, those due to physical limitations of the actuator, cannot be given up and are therefore typically high up in the priority list. Note that although this may not really be considered a case because it is infeasible, we have included it here for the sake of completion.

2.2. Use of Logic to Switch between Active Constraint Regions.

So far we considered the choice of controlled variables for the four different cases of active constraints. In practice, the cases for active constraints change depending on the operating point (disturbances). This results in different operating modes and one way to handle this is to use simple controller logics.

DOI: 10.1021/acs.iecr.9b00308
Ind. Eng. Chem. Res. 2019, 58, 13555−13567

Selectors are commonly used as logic elements when one MV u is used to control several controlled variables (CV) y, i.e., to handle CV−CV switching. In this approach, there is a controller for each CV and the MV-value is selected among the controller outputs using a minimum or maximum selector, depending on the process gains.

Consider for example, two CVs y_i and y_j that needs to be controlled in two neighboring active constraint regions i and j, respectively. Let K_{p_i} and K_{p_j} denote the steady-state process gain from the MV u to the CV y_i and MV u to the CV y_j, respectively. Then switching between y_i and y_j can be achieved using a minimum selector if $sgn(K_{p_i}) = sgn(K_{p_j}) = 1$ or a maximum selector if $sgn(K_{p_i}) = sgn(K_{p_j}) = -1$.

To illustrate this, consider two single loop controllers C_i and C_j with u controlling y_i and the same MV u controlling a different CV y_j, respectively. Let K_i and K_j denote the steady-state controller gain for the two single loop controllers C_i and C_j, respectively. The controller tracking error in this case would then be $e_i = y_i^{sp} - y_i$ for C_i and $e_j = y_j^{sp} - y_j$ for C_j. Consequently, the MV change computed by the two controllers are given by $u = K_i e_i$ and $u = K_j e_j$ respectively.

If the process gain for both the loops are positive (i.e., $sgn(K_{p_i}) = sgn(K_{p_j}) = 1$), then the controller gain for both loops must also be positive. During operation in region i we want the controller tracking error in C_i to be $e_i = 0$, and $e_j > 0$. The control action computed by C_j would then keep increasing due to the integral action. The correct selection would then be the lesser of the two MV value computed by the two controllers. Similarly, during operation in region j we want the controller tracking error in C_j to be $e_j = 0$, and $e_i > 0$. The control action computed by C_i would then keep increasing because of the integral action. The correct selection would again be lesser of the two MV values computed by the two controllers. By the same logic, if the process gain for both the loops are negative (i.e., $sgn(K_{p_i}) = sgn(K_{p_j}) = -1$), then we must select the maximum of the two MV values computed by the controllers, using a maximum selector.

However, If the process gain for the two control loops using the same MV have opposite signs, then the MV change computed by the two control loops would be in the opposite directions. In this case, a minimum or maximum selector would not work and can even lead to unstable response. Therefore, it is important to note that one should never choose to switch between two CV constraints using the same MV if the corresponding process gains have opposite signs. More guidelines on the pairing of the MV and CV are given in the discussions section.

For example, consider a flow line with a valve as the MV. Suppose we have two CVs, namely, to control the flow at its maximum limit and the inlet pressure at its maximum limit. In this case, the flow controller would want to open the valve, whereas the pressure controller would want to close the valve (opposing process gain sign). If a minimum selector is used, it will always choose the pressure controller over the flow controller and similarly, if a max selector is used, the flow controller will always be used. However, if we want to control the pressure at its minimum limit instead, and the flow at its maximum limit, the process gains now have the same sign. Using a minimum selector, the valve will be opened until either the minimum pressure limit is reached or the maximum pressure limit is reached, providing the desired response.

2.3. MV-CV Pairing. When designing simple feedback controllers to achieve optimal operation, another important question that arises is what MVs must be used to control the active constraints and/or the gradient combinations, or in other words, how to pair the MV and CVs to achieve optimal operation and enable switching between the active constraint regions. As for any decentralized control structure design, useful tools such as the relative gain array (RGA) can be used to decide on the CV−MV pairing. Once the different active constraint regions are identified, the corresponding MV−CV pairing must be chosen to design the control loops such that the necessary CVs in each operating regions is controlled by an MV. Hence the active constraint regions play a very important role in choosing the MV−CV pairings. As a rule of thumb, in each active constraint region, the MV−CV pairings must be chosen based on the following:

1. Pair-close rule: to avoid large time delays and sluggish control, it would also be wise to control a CV using an MV that is physically close to it
2. Non-negative RGA: CV−MV pairing must be chosen such that the steady-state RGA of the resulting transfer matrix is non-negative and close to the identity matrix at crossover frequencies.[26]
3. One must also try to avoid pairing important CVs with MVs that quickly saturate[27] and instead pair such MVs with less important CVs that may be given up. Moreover, if we want to switch between two active constraint regions, where the switching is between a CV and MV constraint, then by following this rule, we do not need any additional logics to switch between the CV and MV constraint. In this case, the MV would saturate automatically by giving up on the CV that is no longer active in the new operating region. If this rule is not followed, more logic blocks such as split-range control would be required to re-pair the MV and CV to achieve the same objective, making the control structure unnecessarily complicated.
4. Same process gain sign when using selectors: Another important consideration when choosing the CV−MV pairing is the different combination of the active constraints that must be considered. Once the different possible active constraint regions are identified, selector blocks can be used to switch between two or more CVs using the same MV. When grouping the CVs together that need to be controlled by the same MV, one must not switch between different CVs using the same MV, whose process gain has opposite signs, because the two control loops would be contradictory and working against each other ,as explained in subsection 2.2.

Note that there may be several different possible MV−CV pairings to achieve the same objectives and the pairing rules listed above can guide in selecting a good control structure design that would help reduce the number of logic blocks required to reconfigure the control loops.

3. EXAMPLE 1

To illustrate this, consider a simple toy example with $n_u = 1$ degree of freedom. The optimization problem is given by

$$\min_{\mathbf{u}} J = (\mathbf{u} - \mathbf{d})^2$$
$$\text{s. t.} \qquad (12)$$

DOI: 10.1021/acs.iecr.9b00308
Ind. Eng. Chem. Res. 2019, 58, 13555−13567

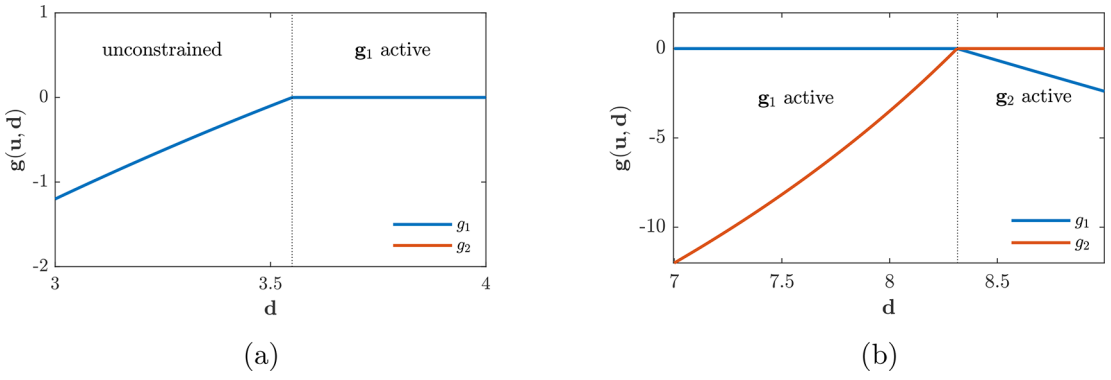

Figure 4. Example 1, optimal constraint values as a function of disturbance. (a) $\mathbf{d} \in [3, 4]$, (b) $\mathbf{d} \in [7, 9]$.

$$\mathbf{g}_1\text{: } (4.8 - 0.4\mathbf{d})\mathbf{u} - 12 \leq 0 \tag{13}$$

$$\mathbf{g}_2\text{: } 5\mathbf{u} + \mathbf{d} - 49 \leq 0 \tag{14}$$

For this problem, we have $n_g = 2$ potential constraints and therefore we can have a maximum of $2^{n_g} = 4$ active constraint regions. These correspond to

- Fully unconstrained (R-I)
- Only $\mathbf{g}_1$ active (R-II)
- Only $\mathbf{g}_2$ active (R-III)
- Both $\mathbf{g}_1$ and $\mathbf{g}_2$ active (infeasible)

Because we only have one MV, we can control at most one CV at any given time. Therefore, the last combination with both constraints active is infeasible and we only need to design controllers for regions R-I, R-II, and R-III.

To better understand the optimal solution (and not because it is necessary for the subsequent controller design), we show the optimal active constraint values for $\mathbf{d} \in [3, 4]$ and $\mathbf{d} \in [7, 9]$ in Figure 4, which was computed by solving the numerical optimization problem offline. It can be seen that, for $\mathbf{d} \leq 3.55$ the problem is unconstrained (R-I) and for $3.55 < \mathbf{d} < 8.3$, constraint $\mathbf{g}_1$ is active (R-II). At $\mathbf{d} = 8.3$, the optimal active constraint switches from g_1 to g_2 (R-III).

The unconstrained optimum for $d \leq 3.55$ is achieved when the cost gradient $\mathbf{J_u} = 0$, which from eq 12 corresponds to $\mathbf{u} = \mathbf{d}$. We therefore propose a control structure with three controllers; one to control the unconstrained optimum ($\mathbf{u} = \mathbf{d}$), and two other to control the constraints g_1 and g_2, respectively. To switch between the three controllers, use a minimum selector logic. The resulting control structure is shown in Figure 5. The simulation results using this control structure are shown in Figure 6.

When using selectors, it is important to note that there will be integral "windup" for the manipulated variable computed by any deselected/inactive controller.[28] A simple remedy to this problem is to use antiwindup logic or bumpless transfer logic[29,30] to avoid any undesired transients when switching between different controllers and controller modes.

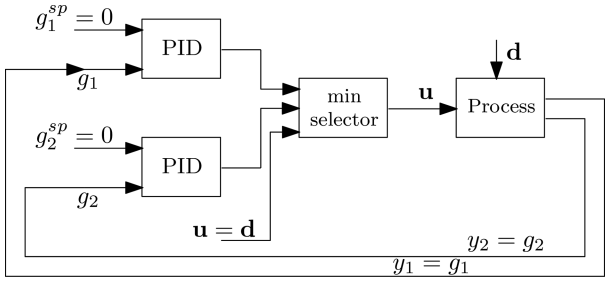

Figure 5. Example 1, block diagram of the control structure to handle changes in the active constraint set.

4. EXAMPLE 2

In this section, we consider optimal operation of a continuously stirred tank reactor (CSTR) from Economou et al.[31] which has been widely studied in academic research.[32−34] The CSTR process has a heater to adjust the feed temperature $u_1 = T_i$ and also the feed rate can be manipulated, $u_2 = F$. There is a reversible exothermic reaction where component A is converted into component B (see Figure 7). The dynamic model of the CSTR is given by two mass balances and one energy balance

$$\frac{dC_A}{dt} = \frac{F}{M}(C_{A,i} - C_A) - r \tag{15a}$$

$$\frac{dC_B}{dt} = \frac{F}{M}(C_{B,i} - C_B) + r \tag{15b}$$

$$\frac{dT}{dt} = \frac{F}{M}(T_i - T) + \frac{-\Delta H_{rx}}{\rho c_p}R \tag{15c}$$

Where the reaction rate is $r = k_1 C_A - k_2 C_B$ with $k_1 = C_1 e^{-E_1/RT}$ and $k_2 = C_2 e^{-E_2/RT}$. C_A and C_B are concentrations of the two components in the reactor whereas $C_{A,i}$ and $C_{B,i}$ are in the inflow. T_i is the inlet temperature, T is the reaction temperature and F is the feed rate. The nominal values for the CSTR process are given in Table. 1.

For this CSTR process, the two degrees of freedom are $\mathbf{u} = [T_i\ F]^T$ and the objective is to maximize a weighted sum of the throughput rate F and the product concentration C_B while penalizing utility costs associated with a high feed temperature T_i. This is subject to maximum feed rate, maximum temperature, and maximum impurity (C_A) constraint. The optimization problem is formulated as

$$\min_{T_i, F} \ -F - 2.009C_B + (1.657 \times 10^{-3} T_i)^2$$

s. t.

$$\mathbf{g}_1\text{: } F/F^{max} - 1 \leq 0$$

$$\mathbf{g}_2\text{: } T/T^{max} - 1 \leq 0$$

$$\mathbf{g}_3\text{: } C_A/C_A^{max} - 1 \leq 0 \tag{16}$$

The concentration of component A in the feed stream $C_{A,i}$ is a disturbance and varies in the range from 0.7 to 1.1mol/L. For

DOI: 10.1021/acs.iecr.9b00308
Ind. Eng. Chem. Res. 2019, 58, 13555−13567

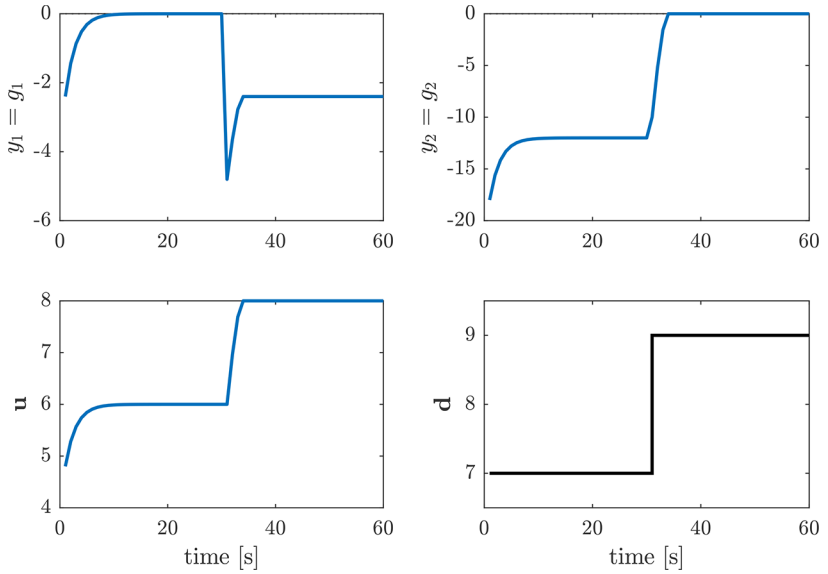

Figure 6. Example 1, simulation results showing the switching between the active constraint regions using a minimum selector block.

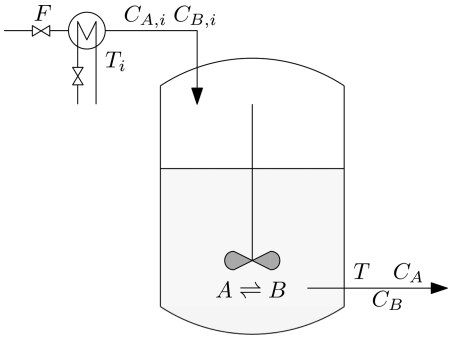

Figure 7. Example 2, exothermic reactor process from Economou et al.[31]

Table 1. Nominal Values for CSTR Process in Example 2

	description	value	unit
F^*	feed rate	1	mol min^{-1}
C_1	constant	5000	s^{-1}
C_2	constant	1×10^6	s^{-1}
C_p	heat capacity	1000	cal kg^{-1} K^{-1}
E_1	activation energy	1×10^4	cal mol^{-1}
E_2	activation energy	15 000	cal mol^{-1}
$C^*_{A,i}$	inlet A concentration	1	mol L^{-1}
$C^*_{B,i}$	inlet B concentration	0	mol L^{-1}
R	universal gas constant	1.987	*cal* mol^{-1} K^{-1}
ΔH_{rx}	heat of reaction	−5000	*cal* mol^{-1}
ρ	density	1	*kg* l^{-1}

this system, we have $n_g = 3$ constraints and $2^3 = 8$ potential active constraint regions, namely

- Fully unconstrained (never)
- only $\mathbf{g}_1$ active (R-I)
- only $\mathbf{g}_2$ active (never)
- only $\mathbf{g}_3$ active (never)
- $\mathbf{g}_1$ and $\mathbf{g}_2$ active (R-II)
- $\mathbf{g}_2$ and $\mathbf{g}_3$ active (R-III)
- $\mathbf{g}_1$ and $\mathbf{g}_3$ active (unlikely)
- $\mathbf{g}_1$, $\mathbf{g}_2$ and $\mathbf{g}_3$ active (infeasible)

Because we only have two MVs, we can have at most two constraints active at any time. Therefore, the potential constraint region 8 listed above is infeasible and can be eliminated. Also, from the cost function in eq 16, the feed rate F will be maximized (i.e., $\mathbf{g}_1$ is active) as long as there are any unconstrained degrees of freedom. This eliminates the fully unconstrained region, the region where only $\mathbf{g}_2$ is active and region where only $\mathbf{g}_3$ are active. Furthermore, based on engineering insight and for the given range of disturbance and activation energy, the reactor temperature constraint ($\mathbf{g}_2$) will become active before the impurity constraint ($\mathbf{g}_3$) becomes active. This eliminates region 7 as unlikely and leaves us with active constraint regions R-I, R-II, and R-III. Solving the numerical optimization problem offline for the expected disturbances confirms that we need to consider the three regions. This is illustrated in Figure 8 which shows the three constraint variables as a function of $C_{A,i}$.

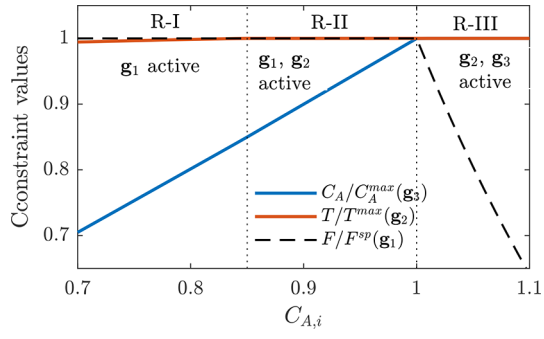

Figure 8. Example 2, optimal constraint values as a function of the disturbance. The three active constraint regions R-I, R-II, and R-III are clearly marked.

In R-I, when $C_{A,i} < 0.85$ mol/L, only the feed rate constraint ($\mathbf{g}_1$) is active, leaving one MV unconstrained. This belongs to the partially constrained case (case 3). Here, we can use the feed rate $u_1 = F$ to maintain the throughput at its constraint value of F^{max} and use the inlet temperature $u_2 = T_i$ to control the gradient $\mathbf{J}_u = \nabla_T J$ (the steady-state gradient from T_i to J) at a constant set point of zero.

This follows from eq 7, which gives

DOI: 10.1021/acs.iecr.9b00308
Ind. Eng. Chem. Res. 2019, 58, 13555−13567

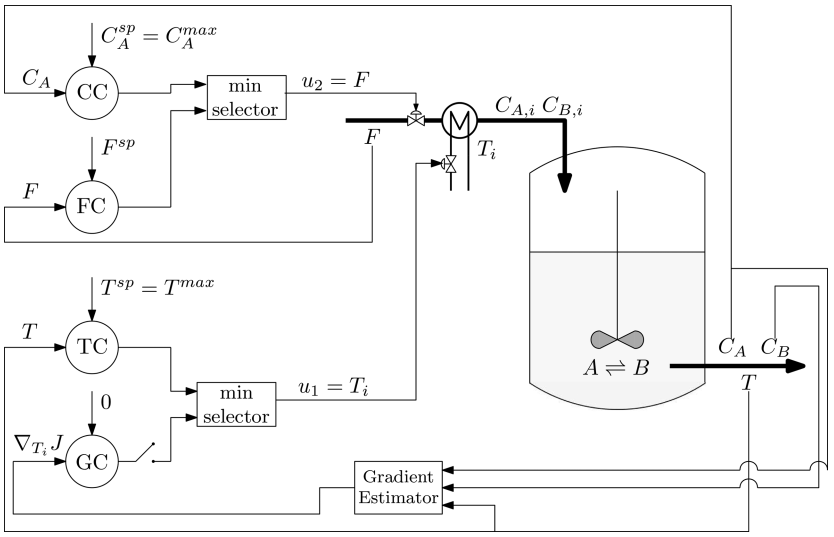

Figure 9. Example 2, proposed control structure design for optimal operation over Regions R-I, R-II, and R-III.

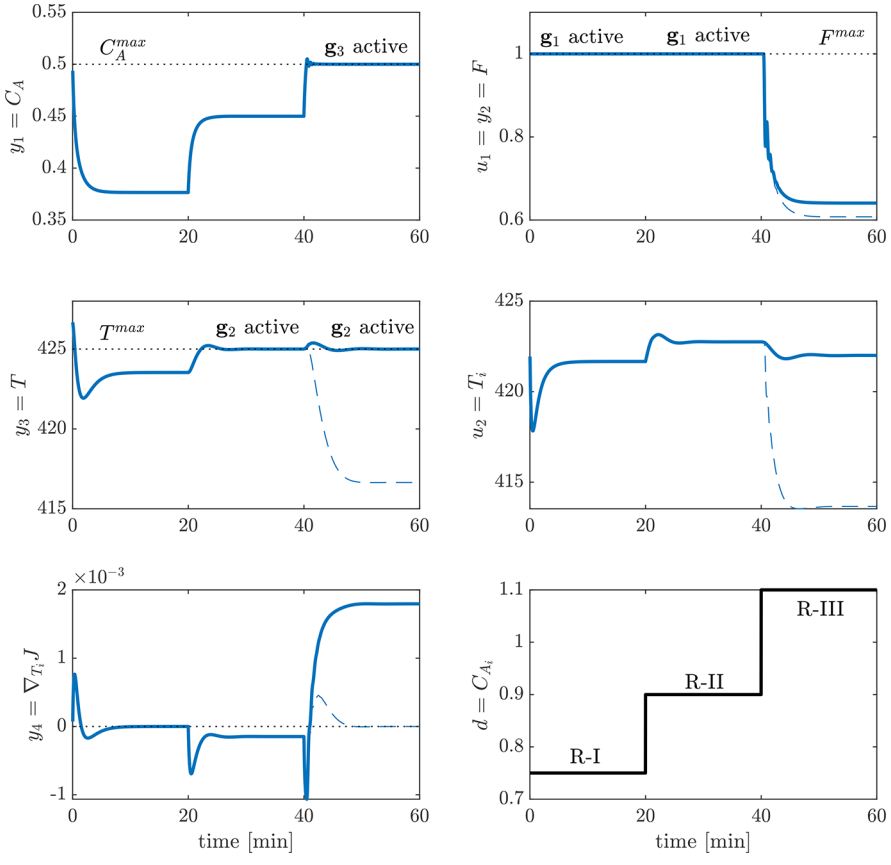

Figure 10. Example 2, simulation results using the proposed control structure (solid thick lines). The thin dashed lines show the simulation results if the GC controller is incorrectly activated in R-III as a motivating example.

$$\begin{aligned} \nabla_{T_i}\mathcal{L} = \; & \nabla_{T_i} J + \lambda \nabla_{T_i}(F - F^{\max}) = 0 \\ \Rightarrow \quad & \nabla_{T_i} J + \lambda \cdot 0 = 0 \\ \Rightarrow \quad & \nabla_{T_i} J = 0 \end{aligned} \tag{17}$$

In this case, we estimate the steady-state gradient $\mathbf{J_u} = \nabla_{T_i} J$ by linearizing a nonlinear dynamic model around the current operating point, as proposed by Krishnamoorthy et al.[17] Note that any gradient estimation method may be used here to estimate the steady-state cost gradient.[22]

In R-II, when $0.85 < C_{A,i} < 1$ mol/L, there are two active constraints, namely, the feed rate ($\mathbf{g}_1$) and the reactor temperature ($\mathbf{g}_2$). This is a fully constrained case (case 2) and we use the feed rate F to maintain the throughput at $F^{\max}$ as in region R-I, and use the inlet temperature T_i to maintain the reactor temperature at its maximum limit.

DOI: 10.1021/acs.iecr.9b00308
Ind. Eng. Chem. Res. 2019, 58, 13555−13567

In R-III, when $C_{A,i} > 1$ mol/L, we also have a fully constrained case with the reactor temperature constraint ($\mathbf{g}_2$) and the product concentration constraint ($\mathbf{g}_3$) being active. The feed rate is no longer at its maximum and is instead used to control the concentration of component A in the outlet less than the maximum limit of 0.5 mol/L to meet the product requirement. As in region R-II, the inlet temperature is used to control the reactor temperature at its maximum limit.

To switch between the different active constraint regions, minimum selector blocks are used. The control structure including the selectors to handle changes in the active constraint is shown in Figure 9. The proposed control structure was tested in simulations with varying values of the disturbance $C_{A,i}$ and the results are shown in Figure 10. All the controllers are PI controllers and are tuned using the SIMC tuning rules.[35] The proportional gain K_C and integral gain K_I are shown in Table. 2.

Table 2. Controller Tunings Used for Example 2 (Figure 9)

	TC	GC	CC	FC
K_C	0.0167	4167	3.3661	0
K_I	0.0167	64.1149	0.2805	1

The simulation starts with $C_{A,i} = 0.75$ mol/L and we can see that the flow controller (denoted FC in Figure 9) maintains the feed rate its set point of $F^{max} = 1$ mol/min and the gradient controller (denoted by GC in Figure 9) drives the system to its optimum. At time $t = 20$ min, the feed concentration changes to $C_{A,i} = 0.9$ mol/L. In this case, the temperature controller (denoted by TC in Figure 9) takes over from the gradient controller and maintains the reactor temperature at its set point of $T^{max} = 425K$. Finally, at time $t = 40$ min, the feed concentration further increases to $C_{A,i} = 1.1$ mol/L. To meet the purity requirement on the product, the concentration controller (denoted by CC in Figure 9) takes over the feed rate control to maintain the concentration of component A at its maximum limit of $C_A^{max} = 0.5$ mol/L by reducing the feed rate.

The true optimal steady-state solution computed by solving a steady-state numerical optimization problem is used as a base case and is compared with the converged solution in Table. 3. By

Table 3. Comparison of the True Optimal Steady-State Solution and the Converged Solution for Example 2

		$C_{A,i} = 0.75$	$C_{A,i} = 0.9$	$C_{A,i} = 1.1$
true optimum	$u_1 = F$	1.000	1.000	0.6408
	$u_2 = T_i$	421.7	422.7	422.0
converged solution	$u_1 = F$	1.000	1.000	0.6408
	$u_2 = T_i$	421.7	422.7	422.0

comparing these simulation results with the true optimal solution, we find as expected that the simple feedback control structure provides optimal operation without needing to solve online numerical optimization problems. The simulation results also demonstrate that simple logics are sufficient to handle changes in active constraint sets without identifying the active constraint regions a priori.

As mentioned earlier, the gradient controller (GC) that controls the steady-state gradient must be inactive in region R-III, because it is not a neighboring region to region R-I. Therefore, one should only to track the gradient in R-I and its neighboring region R-II. One way to do this is by turning off the GC controller when the concentration controller CC that controls C_A becomes active, indicating operation in region 3. Figure 10 also shows as dashed lines, the simulation results when the gradient controller GC incorrectly controls the gradient from R-I also in R-III. This motivates the need for the switch in Figure 9, which turns off the gradient controller in region R-III, when the concentration C_A becomes active. As shown in the simulation results, if the gradient controlled is not turned off in region R-III, we get suboptimal operation with $T < T^{max}$ ($\mathbf{g}_2$ not active as it should be).

Comment: Although the case with $\mathbf{g}_1$ and $\mathbf{g}_3$ active was not relevant for the considered disturbance (and listed as unlikely), it may occur if, for example the activation energy also changes. However, switching to a case where the constraints $\mathbf{g}_1$ and $\mathbf{g}_3$ are active will require a repairing of MVs and CVs, because controllers CC and FC are the two controllers that need to be used in this region and they now both use $u_2 = F$. Additional logics such as split range control logic would be needed to handle this.

5. EXAMPLE 3

In this section, we consider the optimal operation of another CSTR, as studied by Srinivasan et al.[36] and Chachuat et al.[37] It consists of an isothermal CSTR with two exothermic reactions, namely

$$A + B \rightarrow C \tag{18a}$$

$$2B \rightarrow D \tag{18b}$$

The desired product is C, whereas D is an undesired byproduct. The CSTR has two feed streams $u_1 = F_A$ and $u_2 = F_B$ with corresponding known inlet concentrations C_{A_i} and C_{B_i} respectively (see Figure 11).

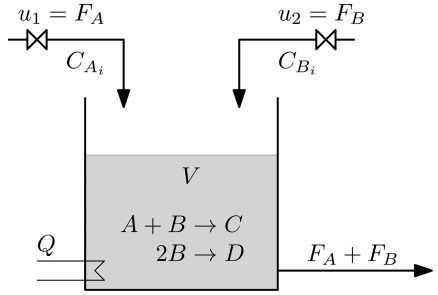

Figure 11. Example 3, isothermal CSTR.[36,37]

We modify the steady-state model from Chachuat et al.[37] to get a dynamic model. Assuming perfect temperature control (isothermal) and level control (constant V), the dynamic model of the process is given by the following material balances:

$$\frac{dn_A}{dt} = F_A C_{A_i} - (F_A + F_B)C_A - k_1 C_A C_B V \tag{19a}$$

$$\frac{dn_B}{dt} = F_B C_{B_i} - (F_A + F_B)C_B - k_1 C_A C_B V - 2k_2 C_B^2 V \tag{19b}$$

$$\frac{dn_C}{dt} = -(F_A + F_B)C_C - k_1 C_A C_B V \tag{19c}$$

where n_A, n_B, and n_C are the number of moles of components A, B, and C, respectively. $C_A = n_A/V$, $C_B = n_B/V$ and $C_C = n_C/V$ are

DOI: 10.1021/acs.iecr.9b00308
Ind. Eng. Chem. Res. 2019, 58, 13555−13567

the concentration of components A, B, and C in the product stream.

The heat produced by the chemical reaction is given by

$$Q = (-\Delta H_1)k_1 C_A C_B V + (-\Delta H_2)k_2 C_B^2 V \quad (20)$$

where ΔH_1 and ΔH_2 denotes the enthalpy of the reactions 1 and 2, respectively. The nominal model parameters are the same as the one used in Chachuat et al.[37] and are shown in Table. 4.

Table 4. Nominal Values for CSTR Process from Example 3.[37]

	description	value	unit
$C^*_{A,i}$	inlet A concentration	2	mol L^{-1}
$C^*_{B,i}$	inlet B concentration	1.5	mol L^{-1}
ΔH_1	enthalpy of reaction 1	-7×10^4	$J\ mol^{-1}$
ΔH_2	enthalpy of reaction 2	-1×10^5	$J\ mol^{-1}$
V	tank volume	500	L
k_1	reaction rate 1	1.5	L mol^{-1} h^{-1}
k_2	reaction rate 2	0.014	L mol^{-1} h^{-1}
F^{max}	maximum flow rate	22	L h^{-1}
Q^{max}	maximum heat	1000	kJ/h

The objective is use feed streams $\mathbf{u} = [F_A\ F_B]$ to maximize the production of component C, which is expressed as the amount of product C, given by the expression, $(F_A + F_B)C_C$ multiplied by the yield factor $(F_A + F_B)C_C/F_A C_{A_i}$.[37] In addition, there are constraints on the cooling Q and the total outflow $(F_A + F_B)$. The optimization problem is then expressed as

$$\min_{F_A, F_B} \quad J = -\frac{(F_A + F_B)^2 C_C^2}{F_A C_{A_i}}$$
$$\text{s. t} \quad (21)$$
$$\mathbf{g}_1\text{: } Q/Q^{max} - 1 \leqslant 0$$
$$\mathbf{g}_2\text{: } (F_A + F_B)/F^{max} - 1 \leqslant 0 \quad (22)$$

Because we have $n_g = 2$ constraints, we have a maximum of $2^2 = 4$ potential active constraint regions, namely,

- Fully unconstrained (unlikely)
- Only $\mathbf{g}_1$ active (R-I)
- Only $\mathbf{g}_2$ active (R-III)
- Both $\mathbf{g}_1$ and $\mathbf{g}_2$ active (R-II)

The reaction rate $d = k_1$ is a disturbance and varies in the range from 0.3 to 1.5 L/(mol h). In this range, the active constraints at the optimum changes with k_1.

Solving numerical optimization problem offline for the expected disturbances show that we only need to consider three different combinations of active constraints; only $\mathbf{g}_1$ active (R-I), both $\mathbf{g}_1$ and $\mathbf{g}_2$ active (R-II), and only $\mathbf{g}_2$ active (R-III). The active constraint regions as a function of the k_1 is shown in Figure 12. It can be seen that there are three active constraint regions, which are marked with R-I, R-II, and R-III, respectively.

In region R-I, when $k_1 < 0.69$, only the outlet flow constraint is active ($\mathbf{g}_2$). This belongs to the partially constrained case (case 3), where we use feed stream $u_1 = F_A$ to control the feed flow $(F_A + F_B)$ at its maximum limit. We use $u_2 = F_B$ to drive the system to its optimum using a gradient controller. Following Theorem 1, expression 8 in this region looks like

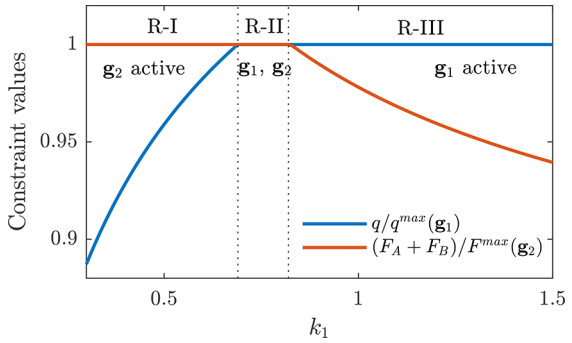

Figure 12. Example 3, optimal values of the normalized constraint variables Q/Q^{max} (solid blue lines) and $(F_A + F_B)/F^{max}$ (solid red lines) as a function of the reaction rate k_1. The three active constraint regions are clearly marked.

$$\nabla_{\mathbf{u}}\mathcal{L}(\mathbf{u}, \mathbf{d}) = \nabla_{\mathbf{u}} J(\mathbf{u}, \mathbf{d}) + \nabla_{\mathbf{u}}(F_A + F_B - F^{max})^T \lambda = 0$$
$$\Rightarrow \begin{bmatrix} \frac{\partial J}{\partial F_A} \\ \frac{\partial J}{\partial F_B} \end{bmatrix} = -\lambda \begin{bmatrix} 1 \\ 1 \end{bmatrix} \quad (23)$$

To eliminate the Lagrange multiplier, we premultiply eq 23 by the nullspace of the active constraint gradients, which in this case is given by $[1\ 1]^T$ and the corresponding nullspace $\mathbf{N} = [-0.7071\ 0.7071]$. This gives the gradient combination

$$\mathbf{c}_1 = \frac{\partial J}{\partial F_A} - \frac{\partial J}{\partial F_B} = 0 \quad (24)$$

Therefore, we use the second degree of freedom to maintain gradient combination $\mathbf{c}_1$ to a constant set point of zero. In this simulation study, we estimate the steady state gradients $\nabla_{\mathbf{u}} J$ by linearizing a nonlinear dynamic model around the current operating point as described by Krishnamoorthy et al.[17]

In region R-II, when $0.69 < k < 0.82$, both constraints $\mathbf{g}_1$ and $\mathbf{g}_2$ are active. This belongs to the fully constrained case (case 2), where optimal operation can be achieved by simply controlling the heat produced to its maximum limit using F_B and the outlet flow rate at its maximum limit using F_A.

In region R-III, when $k > 0.82$, the outlet flow rate constraint is no longer active and only the maximum cooling constraint is active ($\mathbf{g}_1$). This again corresponds to the partially constrained case. Following Theorem 1, expression 8 in this region looks like

$$\nabla_{\mathbf{u}}\mathcal{L}(\mathbf{u}, \mathbf{d}) = \nabla_{\mathbf{u}} J(\mathbf{u}, \mathbf{d}) + \nabla_{\mathbf{u}}(Q - Q^{max})\lambda = 0$$
$$\Rightarrow \begin{bmatrix} \frac{\partial J}{\partial F_A} \\ \frac{\partial J}{\partial F_B} \end{bmatrix} = -\lambda \begin{bmatrix} \frac{\partial Q}{\partial F_A} \\ \frac{\partial Q}{\partial F_B} \end{bmatrix} \quad (25)$$

To eliminate the Lagrange multiplier, we premultiply eq 25 by the nullspace of the active constraint gradients, which in this case is denoted by $\mathbf{N} = [n_1\ n_2]$. This gives the gradient combination of

$$\mathbf{c}_3 = n_1 \frac{\partial J}{\partial F_A} + n_2 \frac{\partial J}{\partial F_B} = 0 \quad (26)$$

DOI: 10.1021/acs.iecr.9b00308
Ind. Eng. Chem. Res. 2019, 58, 13555−13567

Therefore, we use the second degree of freedom $u_2 = F_B$ to maintain gradient combination $\mathbf{c}_3$ to a constant set point of zero.

To switch between the different active constraint regions, minimum selector blocks are used, as shown in Figure 13. The

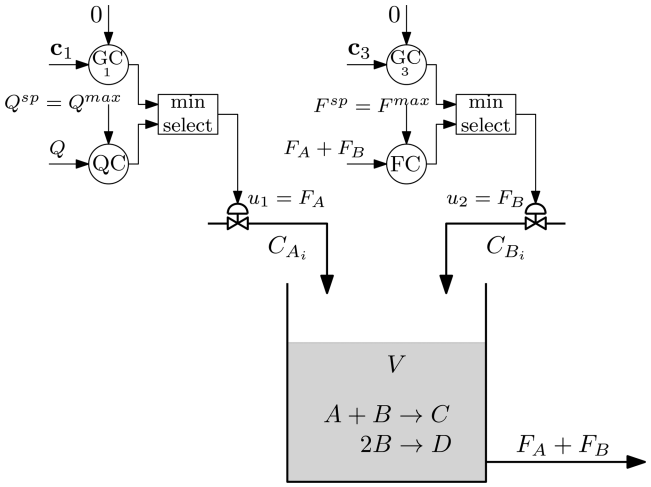

Figure 13. Example 3, proposed control structure design for optimal operation over Regions R-I, R-II, and R-III.

proposed control structure was tested in simulations with varying values of k_1 and shown in Figure 14. All the controllers used in this simulation are PI controllers and are tuned using SIMC tuning rules.[35] The proportional gain K_C and the integral gain K_I for the PI controllers are shown in Table. 5. As

Table 5. Controller Tunings Used in the Controllers Shown in Figure 13

	QC	GC1	GC3	FC
K_C	3.1807	2.1191	2.6647	0
K_I	1.2723	0.0706	0.1665	1

mentioned earlier, the GC1 controller need not be tracked in R-III and similarly GC3 controller need not be tracked in R-I. In other words, GC1 controller can be turned off when GC3 controller is active and vice versa.

The simulation starts in R-III with $k_1 = 1.5$ L/(mol h). In this case, the cooling is maintained at its maximum limit using $u_1 = F_A$ (QC in Figure 13) and the gradient combination $\mathbf{c}_3$ is controlled using $u_2 = F_B$ (GC3 in Figure 13). From time $t = 20$ min, k_1 is ramping down to $k_1 = 0.75$ L/(mol h) to time $t = 40$ min, possibly caused by deactivation of the catalyst. When this happens, the maximum limit on $F_A + F_B$ is reached and the flow control FC takes over from the GC3 controller. The cooling is still maintained at its maximum limit by the QC controller. From time $t = 60$ min, k_1 further ramps down to $k_1 = 0.3$ L/(mol h) to time $t = 80$ min. When this happens, the constraint on the cooling is no longer active and the gradient controller GC1 takes over to maintain the gradient combination $\mathbf{c}_1$ at a constant set point of 0.

The true optimal steady-state solution computed by solving a steady-state numerical optimization problem is used as a base case and is compared with the converged solution in Table. 6. This simulation example shows that simple feedback control structures provide optimal operation without needing to solve online numerical optimization problem. The simulation results

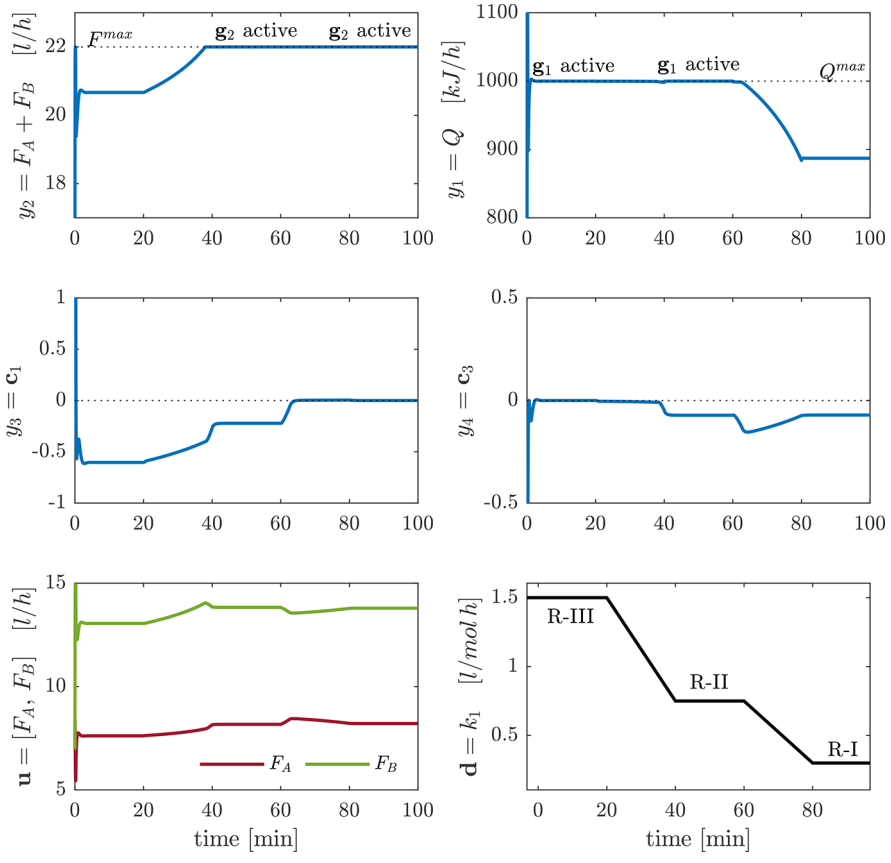

Figure 14. Example 3, simulation results using the proposed control structure.

DOI: 10.1021/acs.iecr.9b00308
Ind. Eng. Chem. Res. 2019, 58, 13555−13567

Table 6. Comparison of the True Optimal Steady-State Solution and the Converged Solution for Example 3

		$k_1 = 1.1$	$k_1 = 0.75$	$k_1 = 0.3$
true optimum	$u_1 = F_A$	7.615	8.171	8.211
	$u_2 = F_B$	13.05	13.83	13.79
converged solution	$u_1 = F_A$	7.615	8.171	8.211
	$u_2 = F_B$	13.05	13.83	13.79

also demonstrate that simple logics are sufficient to handle changes in active CV constraint regions. As mentioned earlier, the GC1 controller that controls the unconstrained optimum in region R-I is turned off in region R-III and similarly, the GC3 controller that controls the unconstrained optimum in region R-III is turned off in region R-I.

Although the fully unconstrained case was not relevant active constraint region for the considered disturbance, this can be easily included in the proposed control structure by adding one more control loop for each MV that controls the steady state gradients $\nabla_{F_A} J$ and $\nabla_{F_A} J$ using $u_1 = F_A$ and $u_2 = F_B$ to a constant set point of zero. The minimum selector box implemented for each MV will then select the minimum of the three controller outputs to be implemented on the process.

6. CONCLUSION

To conclude, using three different examples, we showed that optimal operation of processes can be achieved using simple feedback control structures, without needing to solve computationally intensive optimization problems online. We formalized a framework for optimal control structure design for four different cases, namely, fully constrained, fully unconstrained, partially constrained and over constrained cases. Further, we showed that simple controller logics such as selectors can be used to handle changes in the active constraint regions. In all three different examples, it was shown that a true optimal solution can be obtained using simple feedback controllers despite changes in the active constraint regions.

AUTHOR INFORMATION

Corresponding Author

*Email: skoge@ntnu.no.

ORCID

Dinesh Krishnamoorthy: 0000-0002-9947-8690

Sigurd Skogestad: 0000-0001-6187-8261

Notes

The authors declare no competing financial interest.

ACKNOWLEDGMENTS

The authors gratefully acknowledge the financial support from SFI SUBPRO, which is financed by the Research Council of Norway, major industry partners and NTNU.

REFERENCES

(1) Roberts, P. D.; Williams, T. On an algorithm for combined system optimization and parameter estimation. *Automatica* **1981**, *17*, 199−209.

(2) Marchetti, A.; Chachuat, B.; Bonvin, D. Modifier-adaptation methodology for real-time optimization. *Ind. Eng. Chem. Res.* **2009**, *48*, 6022−6033.

(3) Forbes, J.; Marlin, T.; MacGregor, J. Model adequacy requirements for optimizing plant operations. *Comput. Chem. Eng.* **1994**, *18*, 497−510.

(4) Darby, M. L.; Nikolaou, M.; Jones, J.; Nicholson, D. RTO: An overview and assessment of current practice. *J. Process Control* **2011**, *21*, 874−884.

(5) Krishnamoorthy, D.; Foss, B.; Skogestad, S. Steady-state Real time optimization using transient measurements. *Comput. Chem. Eng.* **2018**, *115*, 34−45.

(6) François, G.; Bonvin, D. Use of transient measurements for the optimization of steady-state performance via modifier adaptation. *Ind. Eng. Chem. Res.* **2014**, *53*, 5148−5159.

(7) Morari, M.; Arkun, Y.; Stephanopoulos, G. Studies in the synthesis of control structures for chemical processes: Part I: Formulation of the problem. Process decomposition and the classification of the control tasks. Analysis of the optimizing control structures. *AIChE J.* **1980**, *26*, 220−232.

(8) Skogestad, S. Plantwide control: The search for the self-optimizing control structure. *J. Process Control* **2000**, *10*, 487−507.

(9) Halvorsen, I. J.; Skogestad, S.; Morud, J. C.; Alstad, V. Optimal selection of controlled variables. *Ind. Eng. Chem. Res.* **2003**, *42*, 3273−3284.

(10) Reyes-Lúa, A.; Zotică, C.; Skogestad, S. Optimal operation with changing active constraint regions using classical advanced control. *IFAC-PapersOnLine* **2018**, *51*, 440−445.

(11) Reyes-Lúa, A.; Zotică, C.; Das, T.; Krishnamoorthy, D.; Skogestad, S. *Comput.-Aided Chem. Eng.* **2018**, *43*, 1015−1020.

(12) Maarleveld, A.; Rijnsdorp, J. Constraint control on distillation columns. *Automatica* **1970**, *6*, 51−58.

(13) Jacobsen, M. G.; Skogestad, S. Active constraint regions for optimal operation of distillation columns. *Ind. Eng. Chem. Res.* **2012**, *51*, 2963−2973.

(14) Arkun, Y.; Stephanopoulos, G. Studies in the synthesis of control structures for chemical processes: Part IV. Design of steady-state optimizing control structures for chemical process units. *AIChE J.* **1980**, *26*, 975−991.

(15) Fisher, W. R.; Doherty, M. F.; Douglas, J. M. The interface between design and control. 3. Selecting a set of controlled variables. *Ind. Eng. Chem. Res.* **1988**, *27*, 611−615.

(16) Kumar, V.; Kaistha, N. Real-Time Optimization of a Reactor-Separator-Recycle Process II: Dynamic Evaluation. *Ind. Eng. Chem. Res.* **2019**, *58*, 1966−1977.

(17) Krishnamoorthy, D.; Jahanshahi, E.; Skogestad, S. A Feedback Real Time Optimization Strategy using a Novel Steady-state Gradient Estimate and Transient Measurements. *Ind. Eng. Chem. Res.* **2019**, *58*, 207−216.

(18) François, G.; Srinivasan, B.; Bonvin, D. Use of measurements for enforcing the necessary conditions of optimality in the presence of constraints and uncertainty. *J. Process Control* **2005**, *15*, 701−712.

(19) Krstić, M.; Wang, H.-H. Stability of extremum seeking feedback for general nonlinear dynamic systems. *Automatica* **2000**, *36*, 595−601.

(20) Hunnekens, B.; Haring, M.; van de Wouw, N.; Nijmeijer, H. A dither-free extremum-seeking control approach using 1st-order least-squares fits for gradient estimation. *IEEE 53rd Annual Conference on Decision and Control (CDC)*; IEEE: 2014; pp 2679−2684.

(21) Dochain, D.; Perrier, M.; Guay, M. Extremum seeking control and its application to process and reaction systems: A survey. *Mathematics and Computers in Simulation* **2011**, *82*, 369−380.

(22) Srinivasan, B.; François, G.; Bonvin, D. Comparison of gradient estimation methods for real-time optimization. *21st European Symposium on Computer Aided Process Engineering-ESCAPE 21*; Elsevier: 2011; pp 607−611.

(23) Jäschke, J.; Skogestad, S. Optimal controlled variables for polynomial systems. *J. Process Control* **2012**, *22*, 167−179.

(24) Alstad, V.; Skogestad, S. Null space method for selecting optimal measurement combinations as controlled variables. *Ind. Eng. Chem. Res.* **2007**, *46*, 846−853.

(25) Manum, H.; Skogestad, S. Self-optimizing control with active set changes. *J. Process Control* **2012**, *22*, 873−883.

(26) Skogestad, S.; Postlethwaite, I. *Multivariable Feedback Control: Analysis and Design*; Wiley & Sons: Chichester, UK, 2005.

DOI: 10.1021/acs.iecr.9b00308
Ind. Eng. Chem. Res. 2019, 58, 13555−13567

(27) Skogestad, S. Control structure design for complete chemical plants. *Comput. Chem. Eng.* **2004**, *28*, 219−234.
(28) Shinskey, F. G. *Process Control Systems: Application, Design and Tuning*, 4th ed.; McGraw-Hill,: New York, 1996.
(29) Hanus, R.; Kinnaert, M.; Henrotte, J.-L. Conditioning technique, a general anti-windup and bumpless transfer method. *Automatica* **1987**, *23*, 729−739.
(30) Graebe, S. F.; Ahlen, A. L. Dynamic transfer among alternative controllers and its relation to antiwindup controller design. *IEEE Transactions on Control Systems Technology* **1996**, *4*, 92−99.
(31) Economou, C. G.; Morari, M.; Palsson, B. O. Internal model control: Extension to nonlinear system. *Ind. Eng. Chem. Process Des. Dev.* **1986**, *25*, 403−411.
(32) Alstad, V. Studies on Selection of Controlled Variables. PhD Thesis, 2005.
(33) Ye, L.; Cao, Y.; Li, Y.; Song, Z. Approximating Necessary Conditions of Optimality as Controlled Variables. *Ind. Eng. Chem. Res.* **2013**, *52*, 798−808.
(34) Jäschke, J.; Skogestad, S. NCO tracking and self-optimizing control in the context of real-time optimization. *J. Process Control* **2011**, *21*, 1407−1416.
(35) Skogestad, S. Simple analytic rules for model reduction and PID controller tuning. *J. Process Control* **2003**, *13*, 291−309.
(36) Srinivasan, B.; Biegler, L. T.; Bonvin, D. Tracking the necessary conditions of optimality with changing set of active constraints using a barrier-penalty function. *Comput. Chem. Eng.* **2008**, *32*, 572−579.
(37) Chachuat, B.; Marchetti, A.; Bonvin, D. Process optimization via constraints adaptation. *J. Process Control* **2008**, *18*, 244−257.

DOI: 10.1021/acs.iecr.9b00308
Ind. Eng. Chem. Res. 2019, 58, 13555−13567